Acta Oceanologica Sinica 2005, Vol. 24, No. 4, p. 54~65
http://www.oceanpress.com.cn
E-mail: hyxbe@263.net

A viscoelastic-plastic constitutive model with Mohr-Coulomb yielding criterion for sea ice dynamics

JI Shunying[1]*, SHEN Hung Tao[2], WANG Zhilian[2], SHEN H Hayley[2], YUE Qianjin[1]

1. State Key Laboratory of Structural Analysis for Industrial Equipment, Dalian University of Technology, Dalian 116023, China
2. Department of Civil and Environmental Engineering, Clarkson University, Potsdam, New York 13699-5710, USA

Received 11 March 2005; accepted 20 April 2005

Abstract

A new viscoelastic-plastic (VEP) constitutive model for sea ice dynamics was developed based on continuum mechanics. This model consists of four components: Kelvin-Vogit viscoelastic model, Mohr-Coulomb yielding criterion, associated normality flow rule for plastic rehololgy, and hydrostatic pressure. The numerical simulations for ice motion in an idealized rectangular basin were made using smoothed particle hydrodynamics (SPH) method, and compared with the analytical solution as well as those based on the modified viscous plastic(VP) model and static ice jam theory. These simulations show that the new VEP model can simulate ice dynamics accurately. The new constitutive model was further applied to simulate ice dynamics of the Bohai Sea and compared with the traditional VP, and modified VP models. The results of the VEP model are compared better with the satellite remote images, and the simulated ice conditions in the JZ20-2 oil platform area were more reasonable.

Key words: sea ice dynamics, constitutive model, viscous plasticity, viscoelastic-plastic model, Mohr-Coulomb criterion

1 Introduction

The motion equation of ice dynamics includes external forces, such as wind and current drags, Coriolis force, gravitational force due to surface gradient force, and the internal ice resistance, which is related to the state of ice field. In a continuum ice dynamics model, it is essential to have a constitutive law. The existing constitutive models for sea ice dynamics mainly include the viscous plastic (VP) model (Hibler, 1979), the elastic plastic (EP) model (Coon et al., 1974; Pritchard, 1975), the viscous elastic plastic model coupled with granular flow dynamics (Shen et al., 1987; Hopkins, 1996), and the anisotropic models (Hibler, 2001; Coon et al., 1998; Pritchard, 1998). The VP model has been applied most widely in the polar areas at large temporal- spatial scale, and the Baltic Sea and Bohai Sea at the meso-scale (Lepparanta and Hibler, 1985; Wu et al., 1998; Zhang, 2000). Different modifications on the VP model have been attempted either for the computational efficiency or for the physical process (Hibler and Schulson, 2000; Flato and Hibler, 1992; Hunke and Dukawicz, 1997; Shen et al., 1990; Ip et al., 1991).

In this paper, a visoelastic-plastic (VEP) model for sea ice dynamics is developed. In this model, the viscous-elastic behavior under small strain and strain rate, the plastic rehology under large strain, the Mohr-Coulomb yielding criterion, and the hydrostatic pressure are considered. Like other VP and EP models, this model also assumes the ice as a two-dimensional isotropic continuum.

To check the validity of the VEP model, the ice ridging process in a rectangular basin and the sea ice

* Corresponding author, E-mail: jisy@dlut.edu.cn

dynamics of the Bohai Sea are simulated. A gridless numerical model using the smoothed particle hydrodynamics (SPH) (Shen et al., 2000; Wang, 2000) is adopted. With its obvious advantage of high precision and numerical diffusion avoided, the SPH method has been applied widely in river and sea ice dynamics in the past decade.

2 Viscoelastic plastic constitutive model for sea ice dynamics

Similar to many constitutive models for ice dynamics, the present model includes a viscoelastic model, a Mohr-Coulomb yielding criterion and a associated normality plastic flow rule. In addition, the hydrostatic pressure depending on the ice thickness is considered.

2.1 Elastic and viscous behavior

Here we use the Kelvin-Vogit model to simulate the ice viscoelastic behavior. Coupling with the plastic rheology, the viscoelastic-plastic model is depicted in Fig.1. The spring, dashpot, and sliding blocks represent the elastic, viscous and plastic properties of sea ice, respectively.

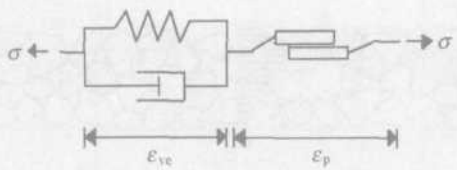

Fig. 1. Viscoelastic-plastic model for sea ice dynamics.

Considering the hydrostatic pressure, the stress-strain relationship of viscoelastic model can be written as

$$\sigma_{ij}=2\eta\varepsilon_{ij}+(\zeta-\eta)\varepsilon_{kk}\delta_{ij}+2G\varepsilon_{ij}+(K-G)\varepsilon_{kk}\delta_{ij}-P_r\delta_{ij}, \quad (1)$$

where ζ_v and η_v are the bulk and shear viscosities; P_r is the horizontal hydrostatic pressure; K and G are the bulk and shear elastic modulus with

$$K=\frac{E}{2(1-\nu)}, \qquad G=\frac{E}{2(1+\nu)}, \quad (2)$$

in which E is the Young's modulus; and ν is the Poisson's ratio.

The elastic modulus of ice cover is affected by ice concentration, based on the concept similar to the formulae of ice strength (Hibler, 1979; Shen et al., 1990). The relationship can be expressed as

$$E=E_0(N/N_{max})^j \quad \text{or} \quad E=E_0e^{-C(1-N)}, \quad (3)$$

where C and j are the empirical constants, normally C= 20 and j=15; N is the ice concentration; N_{max} is its maximum value (Shen et al., 1990; Wang, 2000); and E_0 is Young's modulus. The ice viscosities have the similar relationship with concentration.

2.2 Mohr-Coulomb yielding criterion

The Mohr-Coulomb friction law has been introduced into ice dynamics (Shen et al., 1990; Ip et al., 1991), and it can be written as

$$f(\sigma_1,\sigma_2)=\sigma_1-\sigma_2+(\sigma_1+\sigma_2)\sin\varphi-2c\cos\varphi=0, \quad (4)$$

where c is the cohesion; φ is the ice friction angle; σ_1 and σ_2 are the principle stresses.

The Mohr-Coulomb yield surface is a hexagonal cone in 3-D principle stress space, shown in Fig. 2.

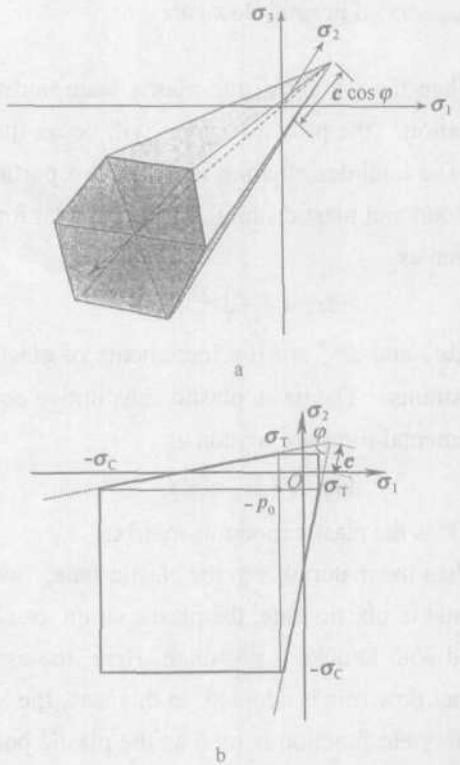

Fig. 2. Mohr-Coulomb yielding criterion.

Generally, when the hydrostatic pressure is non-zero, the principle stress in the z direction $\sigma_3=-P_0$ in which P_0 is the the mean pressure in the vertical direction, a hexagonal curve can be truncated from the hexagonal cone, as shown in Fig. 2b. This yielding function is determined by three parameters, namely, frictional angle, cohesion and hydrostatic pressure. In the EP and VP models, it was set as $P_0=0$ and c=0 respectively (Coon et al., 1998; Ip et al., 1991). The friction angle(φ) may vary with ice conditions. Shen et al. (1990) and Coon et al. (1998) adopted 46° and 52° in river and sea ice simulations. In this paper, we use c=0 and φ=46°, and consider the hydrostatic pressure as well.

The Mohr-Coulomb yield curve is constructed with three couple lines, i.e. shear, compressive and tensile surfaces, and can be written as

$$\sigma_1=K_d\sigma_2+2c\sqrt{K_d}, \tag{5}$$

$$\sigma_C=-K_cP_0-2c\sqrt{K_c}, \tag{6}$$

$$\sigma_T=-K_dP_0+2c\sqrt{K_d}, \tag{7}$$

where $K_d=\tan^2(\pi/4-\varphi/2)$ and $K_c=\tan^2(\pi/4+\varphi/2)$.

2.3 Associated normal flow rule

When the ice enters the plastic state under large deformation, the principle stress will be on the yield curve. The total deformation includes two portions: elastic strain and plastic strain. Its incremental form can be written as

$$d\varepsilon_{ij}=d\varepsilon_{ij}^{e}+d\varepsilon_{ij}^{P}, \tag{8}$$

where $d\varepsilon_{ij}^{e}$ and $d\varepsilon_{ij}^{P}$ are the increments of elastic and plastic strains. The basic plastic constitutive equation in incremental form are written as

$$d\sigma_{ij}=D^{el}(d\varepsilon_{ij}-d\varepsilon_{ij}^{P}) \tag{9}$$

where D^{el} is the elastic modulus matrix.

When the material is in the elastic state, we have $d\varepsilon^{P}=0$, and in plastic state, the plastic strain can be determined with Drucker's postulate. Here, the associated normal flow rule is adopted. In this way, the Mohr-Coulomb yield function is used as the plastic potential function, and the direction of plastic strain rate is normal to the yield curve.

According to the Drucker's postulate and its extensions, the plastic stretching is assumed to be orthogonal to the plastic potential function Ψ, and the plastic strain rate must be directed along the outward normal of Ψ. We may express the normality rule as

$$d\varepsilon_{ij}^{p}=d\lambda\frac{\partial\Psi}{\partial\sigma_{ij}}, \tag{10}$$

where dλ is the plastic multiplier, which can be determined through the consistency condition; Ψ is the plastic potential function, which is set as the yield curve $f(\sigma_{ij})$ in this paper. In the sea ice dynamics, the previous EP (Coon et al., 1974) and VP (Hibler, 1979) models allow non-associated and associated flow rules, respectively.

2.4 Hydrostatic pressure in ice dynamics

In a floating ice field, with gravity and buoyancy, the mean stress in the vertical direction can be calculated as

$$\bar{\sigma}_z=\frac{1}{t_i}\int_{-t_2}^{t_1}\sigma_z dz=\frac{1}{2}\rho_i\left(1-\frac{\rho_i}{\rho_w}\right)gt_i, \tag{11}$$

where ρ_i and ρ_w are the densities of ice and water; $t_i=t_1+t_2$, is the ice thickness, where t_1 and t_2 are the ice thickness above and under the water surface (Fig. 3).

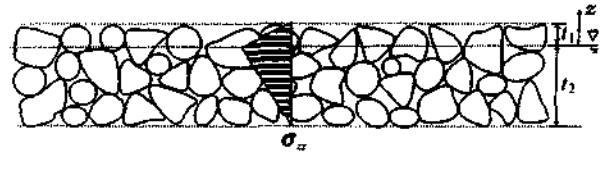

Fig. 3. Hydrostatic pressure in the ice field.

Considering the influence of ice concentration, the mean vertical hydrostatic pressure can be written as (Shen et al., 1990)

$$P_0=\left(1-\frac{\rho_i}{\rho_w}\right)\frac{\rho_i g t_i}{2}\left(\frac{N}{N_{max}}\right)^{j}. \tag{12}$$

The horizontal hydrostatic pressure can be calculated as

$$P_r=K_0P_0, \tag{13}$$

where K_0 is the transfer coefficient, which can be de

termined with experiments. In a broken ice field without cohesion, we have $K_0=1-\sin\varphi$.

3 Numerical simulation of ice ridging in a rectangular basin

Numerical simulation using the present constitutive model is carried out for ice ridging in a rectangular basin. The numerical model is based on the gridless SPH model of Shen et al. (2000). The simulated result is compared with the analytical solution of steady state ridging profile (Pariset et al., 1966).

3.1 Analytical solution of ice ridging

For a rectangular basin with length L and width B covered by uniform layer of ice with initial ice thickness t_{i0} and concentration N_0 (Fig. 4), with constant wind and current drags, the ice cover will pile up at downstream end. The internal ice resistance increases with the ice thickness to balance the wind and current drag forces.

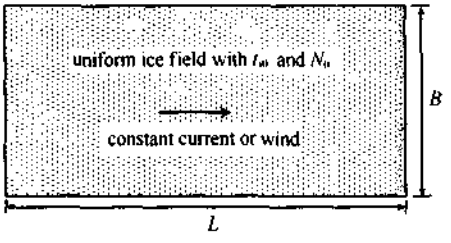

Fig. 4. Definition sketch of ice ridging case.

The momentum equation for ice motion can be written as

$$M\frac{d\mathbf{V}_i}{dt}=-Mf\mathbf{K}\times\mathbf{V}_i+\boldsymbol{\tau}_a+\boldsymbol{\tau}_w-Mg\nabla\xi_w+\nabla(Nt_i\sigma), \quad (14)$$

where M is the ice mass per unit area; $\mathbf{V}_i$ is the ice velocity vector; τ_a and τ_w are the air and water drag stresses;/is the Coriolis paramter; g is the gravitational acceleration; $\nabla\xi_w$ is the ice surface gradient. The air and water drags can be calculated as

$$\left.\begin{aligned}\boldsymbol{\tau}_a&=N\rho_aC_a|\mathbf{V}_{ai}|\mathbf{V}_{ai}\\ \boldsymbol{\tau}_w&=N\rho_wC_w|\mathbf{V}_{wi}|\mathbf{V}_{wi}\end{aligned}\right\}, \quad (15)$$

where C_a and C_w are the wind and current drag coefficients.

At the ice steady ridging state, we have the condition: ice velocity $V_i=0$, strain rate $\varepsilon_{ij}=0$, and ice concentration $N=N_{max}$. Ignoring the gravitational gradient, the ice thickness distribution of static ridge will be analyzed with the traditional VP model, modified VP model and VEP model, respectively.

3.1.1 *Analytical solution without bank friction*

Without bank friction, the 1-D steady state form of Eq. (14) gives

$$N\rho_aC_aV_a^2+N\rho_wC_wV_w^2+\nabla(Nt_i\sigma_{xx})=0, \quad (16)$$

where V_a is the wind velocity; and V_w is the current velocity. The steady ice ridge thickness profile depends on the stress σ_{xx} which can be determined with different constitutive models.

In the traditional viscoplastic model of Hiber (1979), the ice stress equals the pressure term at the steady state, which can be described by

$$\sigma_{xx}=\frac{-P^*}{2}\exp[-C(1-N)]. \quad (17)$$

Substituting Eq. (17) into Eq. (16), the ice thickness profile can be obtained:

$$t_i=t_{i0}+\frac{2(\rho_aC_aV_a^2+\rho_wC_wW_w^2)}{P^*}x, \quad (18)$$

where t_{i0} is the ice thickness at ice edge. In the traditional VP model, the pressure term is independent of ice thickness. Recently, it was improved to $P^*=Ct_i$ considering the ice thickness influence, where C is a constant value (Hibler and Hutchings, 2002) and the P^* is the ice strength in VP model.

In the modified VP model, the pressure term is a linear function of ice thickness (Shen et al., 1990). The ice stress under a convergent state can be written as (Lu and Shen, 1998)

$$\sigma_{xx}=-\tan^2\left(\frac{\pi}{4}+\frac{\varphi}{2}\right)\left(1-\frac{\rho_i}{\rho_w}\right)\frac{\rho_igt_i}{2}\left(\frac{N}{N_{max}}\right)^p. \quad (19)$$

Substituting Eq.(19) into Eq. (16), the ice thickness profile can be calculated by

$$t_i=\sqrt{t_{i0}^2+\frac{2(\rho_aC_aV_a^2+\rho_wC_wV_w^2)}{\tan^2\left(\frac{\pi}{4}+\frac{\varphi}{2}\right)\left(1-\frac{\rho_i}{\rho_w}\right)\rho_ig}x}. \quad (20)$$

For the VEP model, the ice at the edge will not yield, and keeps its thickness. The length of elastic block is dominated by wind stress and compressive strength, and it can be calculated as

$$x_e=\frac{K_c P_0 t_{i0}}{\rho_a C_a V_a^2+\rho_w C_w V_w^2}, \tag{21}$$

where x_e is the length of elastic ice block.

When the ice cover is in the plastic range, the ice stress in x direction can be calculated with Eq. (19), and the ice thickness profile is given by Eq. (20).

3.1.2 *A nalpical solution with bank friction*

When considering the bank friction, the steady ice ridge thickness profile can be obtained from the classical static ice jam theory, which simplifies the problem by averaging the stress in the y direction (Pariset and Hausser, 1966). The stress in x direction is calculated with the plastic limit analytical theory based on the Mohr-Coulomb criterion. The ice ridging height can be calculated as

$$t_i=\sqrt{t_{i0}^2+\frac{B(\rho_a C_a V_a^2+\rho_w C_w V_w^2)}{\rho_i g\tan\varphi(1+\sin\varphi)\left(1-\frac{\rho_i}{\rho_w}\right)}}\times \sqrt{\left[1-\exp\left(-\frac{2(1-\sin\varphi)\tan\varphi}{B}x\right)\right]}. \tag{22}$$

If adopting the VEP model, the length of this elastic zone at the ice edge can be determined as

$$x_e=\frac{K_c P_0 t_{i0}}{\rho_a C_a V_a^2+\rho_w C_w V_w^2-2\mu K_c t_{i0}/B}. \tag{23}$$

In the ice ridging, the ice stress lies on the compressive (convergent) yield surface of Mohr-Coulomb criterion. It is consistent with the classical jam theory. Therefore, the ice ridging profile can also be determined with Eq. (22).

In this ice ridging case, the ice volume remains constant, and the ridging length can be determined according to the thickness profile function. Using the traditional VP model, modified VP model and VEP model, the ice ridging thickness profiles at the steady state are plotted in Fig. 5, and the model parameters are listed in Table 1.

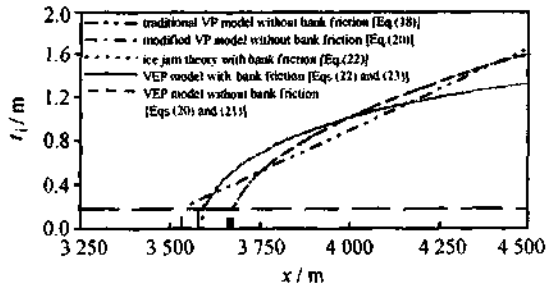

Fig. 5. Analytical solutions of ice thickness profile with different constitutive models.

Table 1. Parameters used in the ice ridging simulation

parameter	Value
t_{i0}/m	0.2
B/m	500
φ/(°)	46
ν	0.3
V_a/m·s^{-1}	15.0
V_w/m·s^{-1}	0.4
C_a	0.015
Δt /s	0.5
N_0	100
L/m	4500
P^*/N·m^{-2}	1.0×10^4
ζ_0/N·s·m^{-2}	1.0×10^8
η_0/N·s·m^{-2}	2.5×10^5
E_0/N·m^{-2}	1.0×10^9
C_w	0.02
ΔS/m	50

Notes: N_0 is the initial ice concentration, ξ_0 is the bulk viscosity, η_0 is the shear viscosity, ΔS is the initial parcel size and Δt is the time step length.

From the analytical solutions, we can find the ice profiles (ridge length, shape, and thickness) analyzed with the VEP model, modified VP model and ice jam theory are very close, in which the ice thickness profile is the quadratic function. It is quite different with the linear function of the traditional VP model.

Moreover, another obvious difference between the VEP model and others is the elastic portion with initial thickness at the upstream ice edge, even it is not so large to affect the ridging profile. The bank friction has an obvious influence on ice the ridging thickness.

3.2 Numerical simulation of ice ridging process

The ice ridging process in a regular basin is simulated with the VEP model. The model parameters in the simulation are listed in Table 1. Considering bank friction, the mean thickness and its contour are plotted in Figs 6 and 7. Under the given wind and current condition, the thickness profile approaches steady state after 2 h. The ice thickness near the bank is thinner than that along the center of the channel. The width-averaged ice thickness is consistent with the analytical solution.

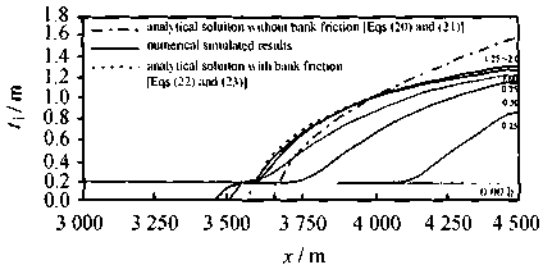

Fig. 6. Width-averaged ice thickness simulated and analytical solution considering bank friction.

The steady state shear and normal stresses in the x direction are presented in Fig. 8. It can be seen that the shear stress is higher at the bank boundary, approaches zero at the middle basin, and is symmetric with the centerline. The normal stress in the % direction is proportional to the ice thickness.

4 Simulation of Bohai Sea sea ice

To examine the validity of VEP model, we simulate the sea ice dynamics of Bohai Sea, and compare its results with those of the traditional VP model (Hibler, 1979) and modified VP model (Shen et al., 1990).

4.1 Input data

In the simulation of Bohai Sea sea ice dynamics, the input data includes the initial ice field, wind and current conditions. The initial ice thickness and concentration are estimated from the NOAA satellite images. The satellite image and the initial ice thickness (14:13, January 21, 1998) are shown in Fig. 9. In the following 48 h simulation, the input wind field can be determined with an operational atmospheric model (Wang, 2000). The tidal current is simulated with a 2-D shallow water equation solved by the ADI finite difference method (Zhang, 2000). In the ice dynamics simulation, the SPH method is adopted (Wang, 2000). The major parameters are listed in Table 1, and some modified parameters according to Bohai Sea sea ice conditions are listed in Table 2.

Table 2. Some parameters used in the sea ice dynamics simulation of the Bohai Sea

Parameter	Value
C_0	0.001 5
C_w	0.002 5
P'/N·m^{-2}	5 000
ζ_{max}/N·s·m^{-2}	1.0×10^{10}
Δt/s	40
ΔS/km	2

Notes: ξ_{max} is the maximum bulk viscosity.

4.2 Simulated results of ice field

With the traditional VP, modified VP and VEP models, the simulated ice thickness, concentration, velocity and principle stress in 24 and 48 h are plotted in Figs 10~12. Under the strong tidal current action, the ice velocities simulated with different models are very close. From the ice principle stress, the results of the VEP model and modified VP model are similar, for their stresses are both dependent on the ice thickness. In this simulation of the traditional VP model, the pressure term P*=5 kN/m^2. Even it is much smaller than that used in the polar areas, the stress calculated is still far higher than that of the VEP model and modified VP model.

From the comparison between the satellite remote image and the simulated ice thickness distribution (see Fig. 13), we can find that the simulated results of the

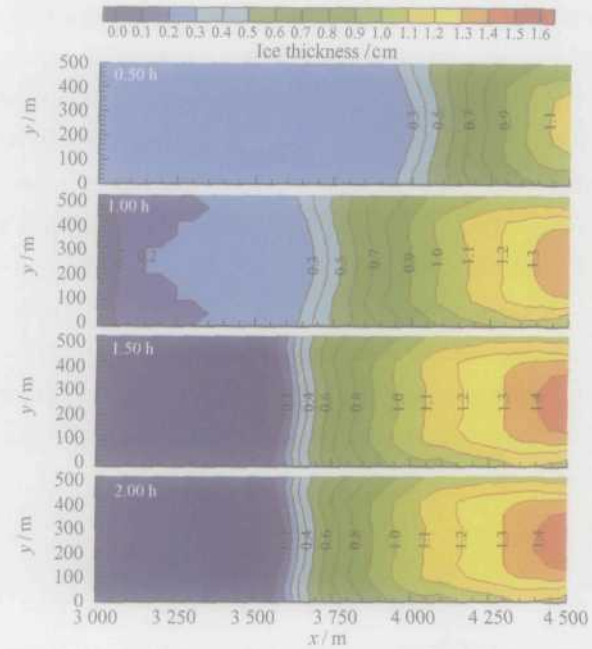

Fig. 7. Ice thickness contour simulated with the VEP model.

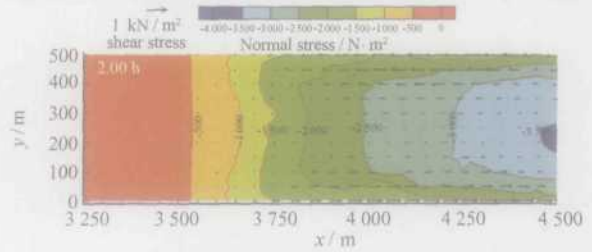

Fig. 8. Distribution of shear stress and normal stress in the *x* direction.

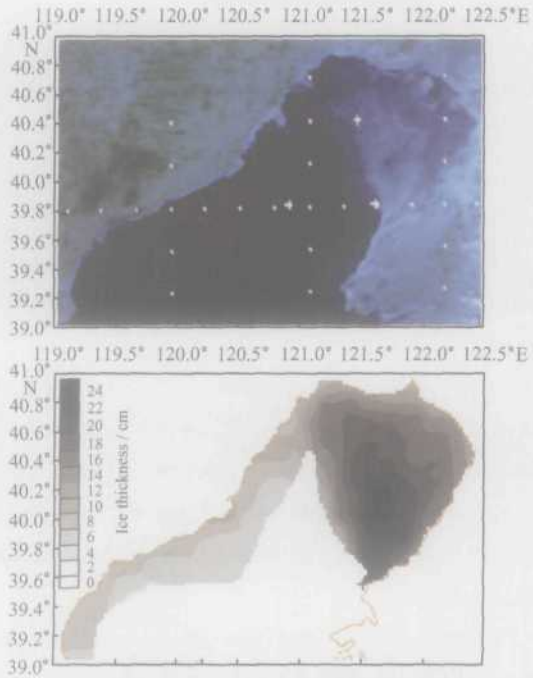

Fig. 9. Satellite remote-sensing image and initial ice thickness distribution (14:13, January 21, 1998).

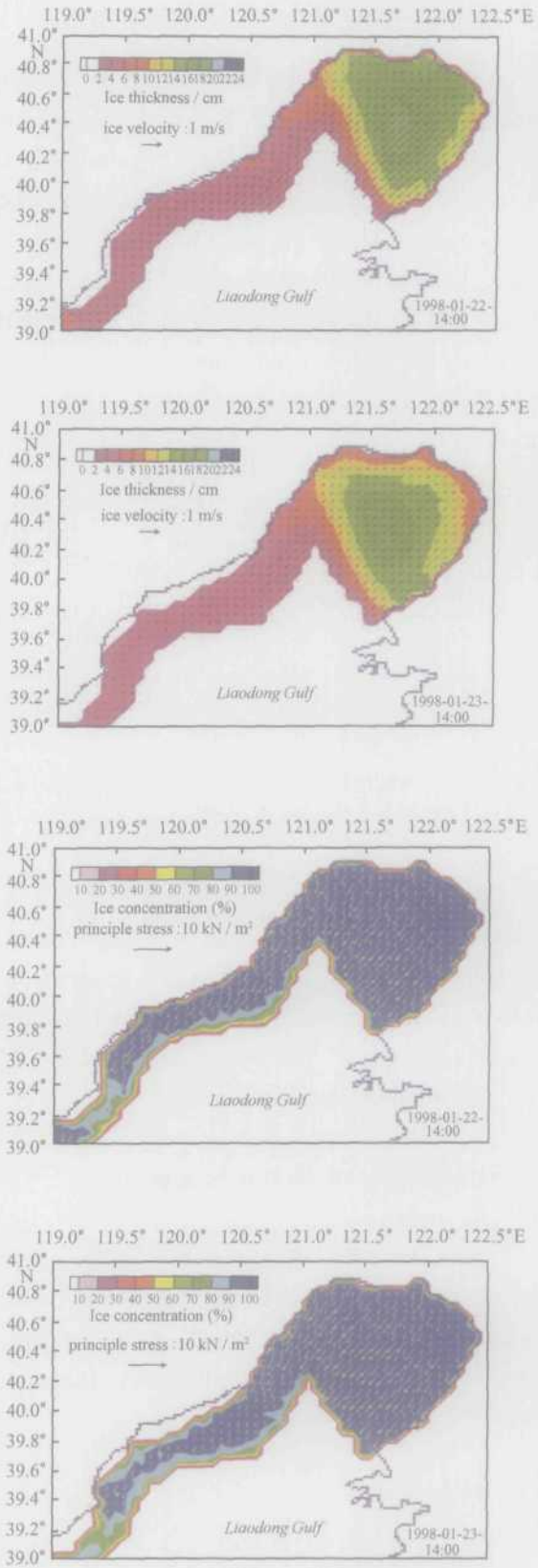

Fig. 10. Ice thickness, concentration, velocity and principle stress simulated with the traditional VP model.

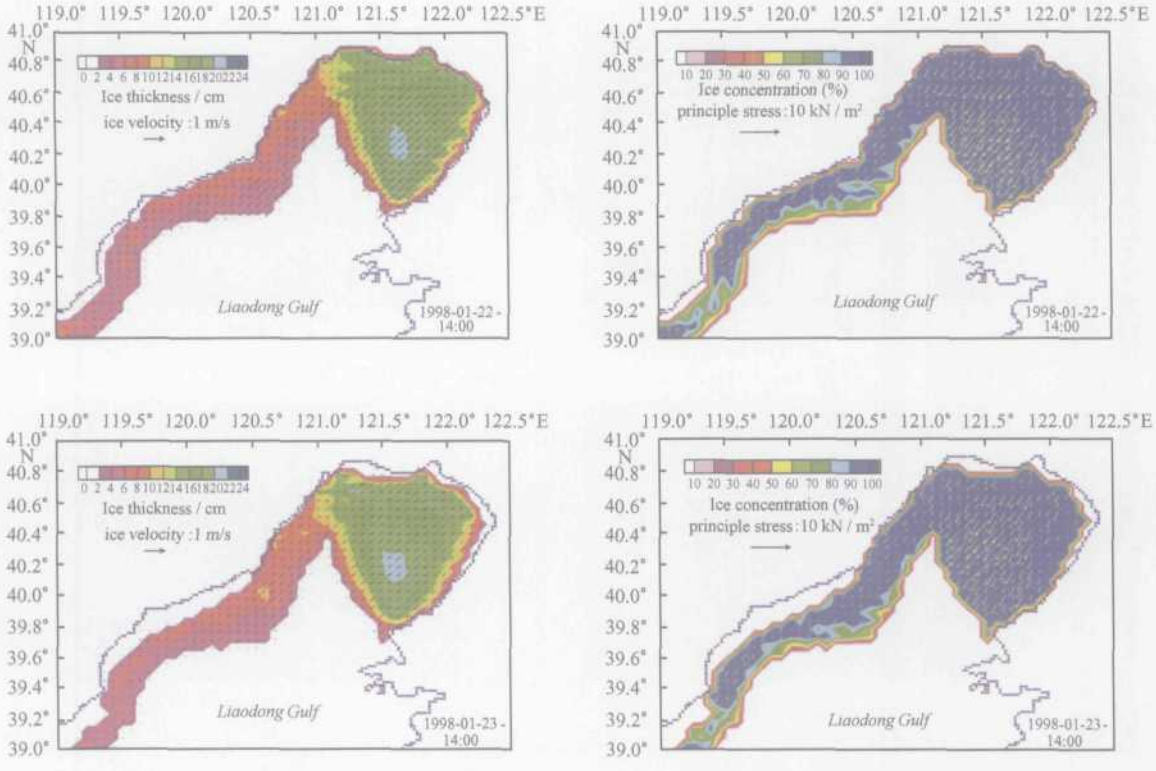

Fig. 11. Ice thickness, concentration, velocity and principle stress simulated with the modified VP model.

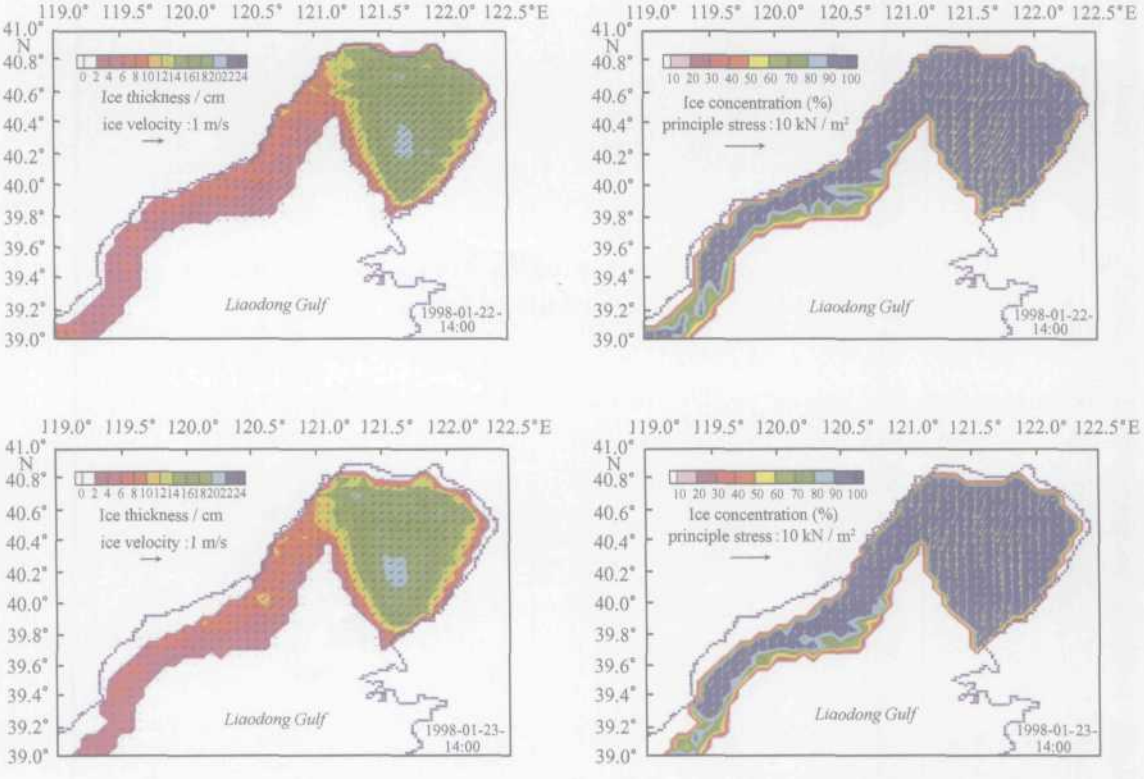

Fig. 12. Ice thickness, concentration, velocity and principle stress simulated with the VEP model.

Fig. 13. Satellite remote image and ice thickness contours at 24 and 48 h simulated with the traditional VP, modified VP and VEP models.

three models above are all consistent with the real ice conditions. The result of modified VP model has two characteristics of the traditional VP model and VEP model. The one is the ice ridging in east area by the traditional VP model, and the other is the heavy thickness distribution in the low middle area by the VEP model. The main reason is the modified VP model has the same elliptical yield curve as the traditional VP model, and also has the similar ice strength as the VEP model. The ice edge simulated with the VEP model is more accurate than others.

4.3 Simulated results at JZ20-2 area

At the JZ20 -2 Oil/Gas Field of the Liaodong Gulf, the ice conditions, such as the ice thickness, velocity, stress and convergence, etc., are interpolated from its neighbor ice parcels with Gaussian function (see Figs 14~18). The ice thickness simulated with the VEP and modified VP models is more similar than that of the traditional VP model (Fig. 14). The ice velocities with the three models are very close as the ice drifting is mainly controlled by the tidal current (Fig.

15). The divergences of ice velocity simulated with the VEP model and the modified VP model fluctuate with the tidal current regularly, but those of the traditional VP model has a strong random fluctuation (Fig. 16). The similar phenomena appear in the stresses (Fig. 17). The stress magnitudes simulated with the VEP model and the modified VP model are very close, and they are much lower than those of the traditional VP model obviously. If we reduce the pressure term P^* of the traditional VP model from 5.0 to 1.0 kN/m^2, the regular fluctuation of ice stress and velocity divergence can also be obtained. From the principle stress of the three models (Fig. 18), we can find that the ice cover shows to be plastic behaviors no matter which model is applied.

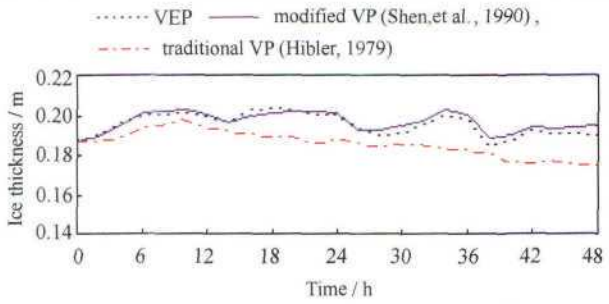

Fig. 14. Ice thickness simulated in 48 h in the JZ20-2 area.

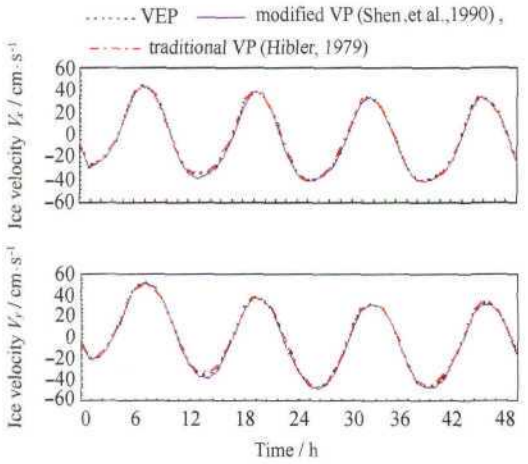

Fig. 15. Ice velocity simulated in 48 h in the JZ20-2 area.

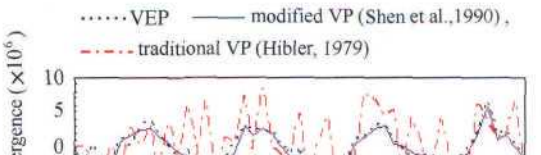

Fig. 16. Velocity divergence simulated in 48 h in the JZ20-2 area.

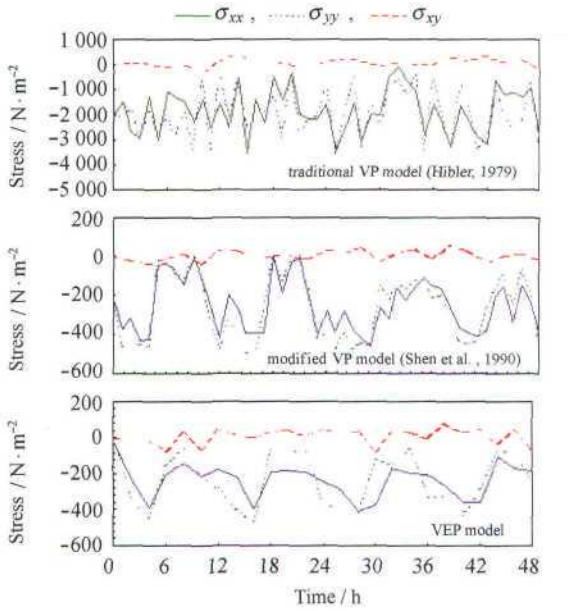

Fig. 17. Stresses of sea ice simulated in 48 h in the JZ20-2 area.

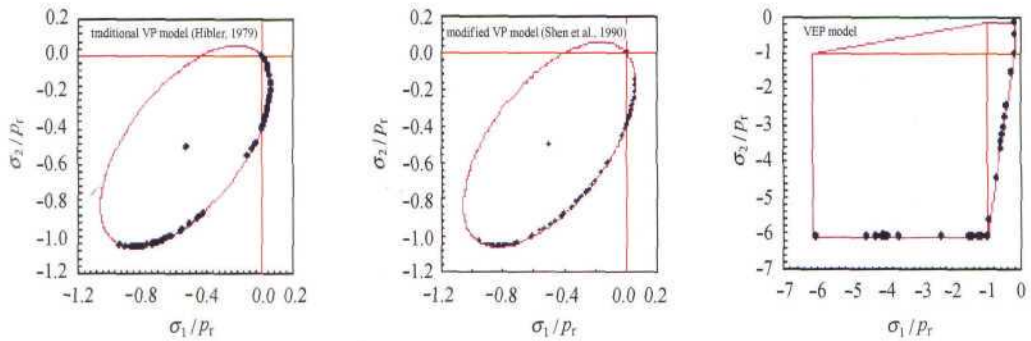

Fig. 18. Principle stress state of sea ice simulated in the JZ20-2 area.

5 Conclusions

A comprehensive viscoelastic-plastic (VEP) constitutive model was presented to improve the precision of sea ice dynamics simulation at the meso-small scale. In this VEP model, the viscoelastic behavior before yielding, plastic rehology beyond yielding of ice cover are both considered. The Mohr-Coulomb yielding criterion, the associated normality plastic flow rule and the hydrostatic pressure in the ice jam theory are all adopted. With this VEP model, the ice ridging process in a rectangle basin was simulated validly. The simulated ice thickness profile at a steady state is agreeable with the analytical solutions of the modified VP model (Shen et al., 1990) and the classical ice jam theory (Pariset et al., 1966). Moreover the ice dynamics of the Bohai Sea was simulated in 48 h with the VEP model, the traditional VP model and the modified VP model, respectively. From the comparison of the simulated ice thickness with the satellite remote images, it is found that the present VEP model can simulate the ice edge and the ice thickness distribution more accurately. The stability of the VEP model was also verified with the simulated ice parameters in the JZ20-2 area. In the VEP model, some parameters, such as the viscosity, the elastic modulus, the cohesion, etc., should be adjusted under different ice conditions.

Acknowledgements

The authors would like to acknowledge the supports by the National Natural Science Foundation of China under contract No. 40206004, and partly by the East-Asia and Pacific Program of US National Science Foundation under contract No. INT-9912246.

References

Coon M D, Knoke G S, Echert D C, et al. 1998. The architecture of an anisotropic ealsitc-plastic sea ice mechanics constitutive law. Journal of Geophysical Research, 103 (C10): 21 915~21 925

Coon M D, Maykut S A, Pritchard R S, et al. 1974. Modeling the pack ice as an elastic plastic material. AIDJEX Bull, 1974,24: 1~105

Flato G M, Hibler W D. 1992. Modeling pack ice as a cavitating fluid. Journal of Physical Oceanography, 22: 626~651

Hibler W D. 1979. A dynamic thermodynamic sea ice model. Journal of Geophysical Oceanography, 9: 817~846

Hibler W D. 2001. Sea ice fracturing on the large scale. Engineering Fracture Mechanics, 68: 2 013~2 043

Hibler W D, Hutchings J K. 2002. Multiple equilibrium arctic ice cover states induced by ice mechanics. Ice in the Environment: Proceedings of the 16th IAHR International Symposium on the ice. Dunedin, New Zealand: University of Otago, 40~45

Hibler W D, Schulson E M. 2000. On modeling the anisotropic failure and flow of flawed sea ice. Journal of Geophysical Research, 105(C7): 17 105~17 120

Hopkins M A. 1996. On the mesosacle interaction of lead ice and floes. Journal of Geophysical Research, 101 (C8): 18 315~18 326

Hunke E C, Dukowicz J K. 1997. An elastic-viscous-plastic model for sea ice dynamics. Journal of Physical Oceanography, 27: 1 849~1 867

Ip C F, Hibler W D, Flato G M. 1991. On the effect of the rheology on seasonal sea ice simulations. Ann Glaciol, 15: 17~25

Lepparanta M, Hibler W D. 1985. The role of plastic ice interaction in marginal ice zone dynamics. Journal of Geophysical Research, 90(C6): 11 899~11 909

Lu S, Shen H T. 1998. Constitutive laws for river ice dynamics. In: Shen H T, ed. Ice in Surface Water. Rotterdam: Balkema, 109~116

Pariset E, Hausser R, Gagnon A. 1966. Formation of ice cover and ice jams in rivers. Journal of Hydraulics Division, ASCE, 92(HY6):1~24

Pritchard R S. 1975. An elastic-plastic constitutive law for sea ice. Journal of Applied Mechanics, 42: 379~384

Pritchard R S. 1998. Ice conditions in an anisotropic sea ice dynamics model. International Journal of Offshore and Ploar Engineering, 8: 9~15

Shen H H, Hibler W D, Lepparanta M. 1987. The role of floe collisions in sea ice rheology. Journal of Geophysical Research, 94(C10): 14 525~14 537

Shen H T, Shen H H, and Tsai S M. 1990. Dynamic transport of river ice. Journal of Hydraulic Research, 28(6):659~671

Shen H T, Su J, Liu L W. 2000. SPH simulation of river ice dynamics. Journal of Computational Physics, 165:752~770

Tremblay L B, Mysak L A. 1997. Modeling sea ice as a granular material, including the dilatancy effect. Journal of Physical Oceanography, 27: 2 342~2 360

Ukita J, Moritx R E. 1995. Yield curves and flow rules of pack ice. Journal of Geophysical Research, 100: 4 545-4 557

Wang Z L. 2000. A coastal sea ice model with discrete parcel method. Clarkson University Internal Report, n 99-16. Potsdam: Clarkson University, 146

Wu Huiding, Bai Shan, Zhang Zhanhai. 1998. Numerical simulation for dynamical processes of sea ice. Acta Oceanologica Sinica, 16(3): 303~325

Zhang Z H. 2000. On modeling ice dynamics of semi-enclosed seasonally ice-covered seas. Report Series in Geophysics. Helsinki: Finnish Institute of Marine Research